Laterally Linked Liquid Crystal Dimers with Electrooptic Properties

David R. Medeiros, Michael A. Hale, Jeffrey K. Leitko, and C. Grant Willson*

Departments of Chemistry and Chemical Engineering, The University of Texas at Austin, Austin, Texas 78751

Received December 1, 1997. Revised Manuscript Received March 16, 1998

Unusual electric field induced phase transitions have been demonstrated in laterally linked smectic C liquid crystals that possess two chiral carbons. The materials have a rich polymorphism including an apparent antiferroelectric phase which occurs at temperatures immediately below the smectic A to C transition. Another tristable phase has been observed closer to the smectic C to crystal transition. The temperature-dependent electrooptic response and spontaneous polarization measurements for the title compounds are compared with those of monomeric liquid crystals of similar structure. The synthesis and characterization of these compounds are also presented in detail.

Introduction

As the demand increases for higher resolution and greater viewing angle in flat panel liquid crystal displays (LCDs), researchers are expanding their investigations beyond the conventional nematic liquid crystals and twisted nematic displays (TNDs) and have begun developing devices based on chiral smectics. The ferroelectric behavior exhibited by chiral tilted smectic (S_C*) liquid crystals[1] has prompted a great deal of interest in the development of new materials directed toward applications in fast electrooptics.[2] The optical anisotropy of these rodlike mesogens, coupled with their propensity to self-assemble and to be reoriented by external stimuli, leads to the usefulness of these materials in light modulation.[3,4] It is their memory, or bistability, an inherent property of ferroelectrics, which makes these materials so desirable. This property allows for the use of passive matrix addressing and, therefore, cheaper manufacturing costs than active matrix nematic displays. Recent commercialization[5] of devices based on the prototype surface-stabilized ferroelectric liquid crystal (SSFLC) device created by Clark and Lagerwall[6] is testament to this trend toward faster, high-contrast electrooptics. However, it is the requirement of robust surface stabilization which some see as a limiting factor in the wide acceptance of this type of display.

Within the past decade, antiferroelectric liquid crystals (AFLCs) have been reported which exhibit tristable switching.[7−14] Experimental displays based on these materials are not as dependent on the surface anchoring required in the SSFLC and exhibit self-recovery from mechanical shock.[7] These materials have therefore garnered the interest of numerous chemists, who are preparing new materials, and condensed matter physicists, who are exploring the fundamental physical aspects of this unique mesophase.

Ferroelectric and antiferroelectric switching are observable in low molecular mass compounds,[4,7−13] in polymers containing mesogenic pendant groups,[14−16] and in dispersions of these compounds in polymer matrixes.[17,18] As the number of known AFLC materials has increased, empirical guidelines have evolved to guide molecular engineering of materials with this property.[2,8,9] We have incorporated many of these concepts for imparting AF behavior into the design of a laterally methylene linked dimeric liquid crystal, **1** (Figure 1), similar in structure to the Schiff's base dimers first proposed by A. C. Griffin and co-workers.[19−21]

(1) Meyer, R. B.; Liebert, L.; Strzelecki, L.; Keller, P. *J. Phys.* **1975**, *36*, 69.
(2) Patel, J. S. *Annu. Rev. Mater. Sci.* **1993**, *23*, 269.
(3) Walba, D. M. *Science* **1995**, *270*, 250.
(4) Goodby, J. W. *Science* **1986**, *231*, 350.
(5) (a) Handschy, M.; Locke, C. *Adv. Imaging* **1997**, *12* (1), 10. (b) Carothers, B. *Electron. News* **1992**, *32* (23), 20. (c) Freemantle, M. *Chem. Eng. News* **1996**, *74*(51), 33.
(6) Clark, N. A.; Lagerwall, S. T. *Appl. Phys. Lett.* **1980**, *36*, 899.
(7) Fukuda, A.; Takanishi, Y.; Isozaki, T.; Ishikawa, K.; Takezoe, H. *J. Mater. Chem.* **1994**, *4*, 997.
(8) Goodby, J. W.; Patel, J. S.; Chin, E. *J. Mater. Chem.* **1992**, *2*, 197.
(9) (a) Goodby, J. W.; Leslie, T. M. *Mol. Cryst. Liq. Cryst.* **1984**, *110*, 175. (b) Gray, G. W.; Goodby, J. W. *Mol. Cryst. Liq. Cryst.* **1976**, *37*, 157.
(10) (a) Johno, M.; Chandani, A. D. L.; Ouchi, Y.; Takezoe, H.; Fukuda, A.; Ichibashi, M.; Furukawa, K. *Jpn. J. Appl. Phys., Part 2* **1989**, *28*, L119. (b) Chandani, A. D. L.; Ouchi, Y.; Takezoe, H.; Fukuda, A.; Terashima, K.; Furukawa, K.; Kishi, A. *Jpn. J. Appl. Phys., Part 2* **1989**, *28*, L1261.
(11) Chandani, A. D. L.; Hagiwara, T.; Suzuki, Y.; Ouchi, Y.; Takezoe, H.; Fukuda, A. *Jpn. J. Appl. Phys.* **1988**, *27*, L729.
(12) Byron, D. J.; Komitov, L.; Matharu, A. S.; McSherry, I.; Wilson, R. C. *J. Mater. Chem.* **1996**, *6*, 1871.
(13) Booth, C. J.; Dunmur, D. A.; Goodby, J. W.; Toyne, K. J.; Watson, M. J. *J. Mater. Chem.* **1996**, *6*, 919.
(14) Nishiyama, I.; Goodby, J. W. *J. Mater. Chem.* **1993**, *3*, 169.
(15) Sahlén, F.; Trollsås, M.; Hult, A.; Gedde, U. W. *Chem. Mater.* **1996**, *8*, 382.
(16) Kuehnpand, K.; Springer, J. *Makromol. Chem. Rapid Commun.* **1991**, *12*, 127.
(17) Chiellini, E.; Galli, G.; Cioni, F.; Dossi, E. *Makromol. Chem., Macromol. Symp.* **1993**, *69*, 51.
(18) Nishiyama, I.; Yoshizawa, A. *Ferroelectrics* **1996**, *179*, 103.

S0897-4756(97)00764-3 CCC: $15.00
Published on Web 05/30/1998

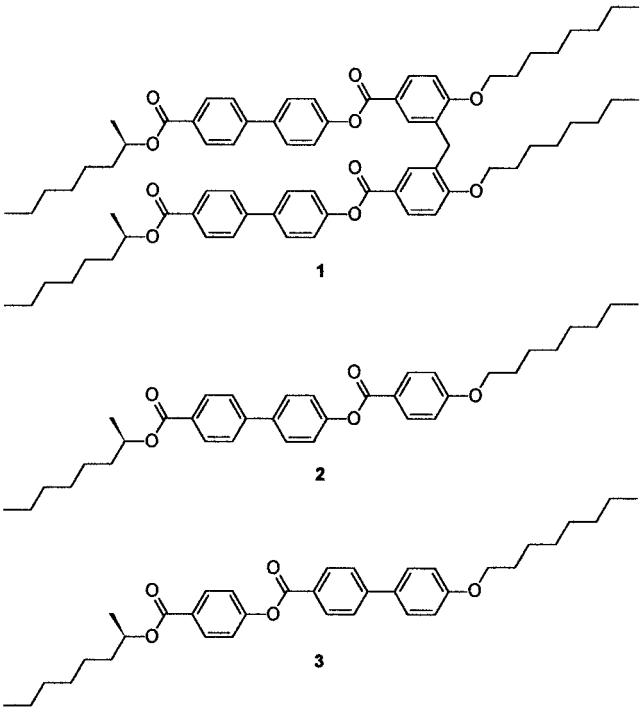

Figure 1. Molecular structures of laterally linked dimer **1**; its corresponding monomer, **2**; and MHPOBC, **3**.

This paper reports the fundemental investigations of this new type of dimeric electrooptic liquid crystal.

The dimeric material, **1**, comprises two "monomers" of 1-methylheptyl 4″-(4′-(octyloxy)benzoyl)oxy)biphenyl-4-carboxylate, **2**, that are symmetrically linked through a methylene spacer attached to each monomer's rigid core. The chiral smectogen, **2**, first reported by J. W. Goodby and co-workers,[8] is a constitutional isomer of 4-(((1-methylheptyl)oxy)carbonyl)phenyl 4′-(octyloxy)-biphenyl-4-carboxylate, **3**, often referred to as MHPOBC. MHPOBC was among the first liquid crystalline materials shown to exhibit antiferroelectric behavior[10,11] and often serves as a benchmark to which other FLC and AFLC compounds are compared. In this study we contrast the polymorphism and electrooptic properties of dimer **1** with those of both monomer **2** and MHPOBC **3**.

Experimental Section

Reagents and Chemicals. All chemicals were obtained from Aldrich Chemicals and used as received unless noted otherwise. THF was distilled from NaK/benzophenone ketyl prior to use. Toluene was distilled from sodium. Methylene chloride was distilled from calcium hydride. Pyridine was dried over activated 4-Å molecular sieves and distilled. Thionyl chloride was twice distilled, first from linseed oil, then neat. Merck grade 9385 silica gel (230−400 mesh, 60 Å) was used for all column chromatography separations. MHPOBC was purchased from Aldrich.

Synthesis. *4,4′-Dihydroxy-3,3′-methanediyldibenzoic Acid, Dimethyl Ester, **4***. Methyl 4-hydroxybenzoate (20.0 g, 132 mmol) was partially dissolved in 350 mL of 50% (v/v) H_2SO_4 in a round-bottom flask and heated to 80 °C. A 37 wt. % aqueous solution of formaldehyde (2.27 g, 28.0 mmol) was added dropwise to the cloudy solution. The mixture was allowed to stir for 2 h at 80 °C. The resulting slurry was cooled to room temperature, and the white solid was collected and washed repeatedly with water. The crude product was slurried several times in ethyl acetate to remove unreacted starting material. The insoluble material was dried to constant weight to yield 7.40 g (84%) of the desired product; mp 259−261 °C. ^{1}H NMR (DMSO-d_6): δ 3.73 (s, 6H, CO_2CH_3), 3.85 (s, 2H, $ArCH_2Ar$), 6.89 (d, J = 7.8 Hz, 2H, Ar*H*), 7.62 (s, 2H, Ar*H*), 7.68 (d, J = 7.8 Hz, 2H, Ar*H*), 10.42 (bs, 2H, O*H*).

*4,4′-Dioctyloxy-3,3′-methanediyldibenzoic Acid, Dimethyl Ester, **5***. In a round-bottom flask 2.35 g (7.44 mmol) of **4** was dissolved in 20 mL of DMSO. K_2CO_3 (2.49 g, 18.0 mmol) was added, and the mixture was stirred under N_2. 1-Iodooctane (3.84 g, 16.0 mmol) was added, and the solution was heated to 75 °C and allowed to stir for 48 h. The reaction mixture was cooled to room temperature and diluted with 50 mL of water. The organics were extracted with several small portions of toluene. The combined organic fractions were washed with water and dried over Na_2SO_4. Removal of the solvent afforded a crude solid, which was recrystallized twice from hexanes/ethyl acetate (15/1) to give 2.75 g (68%) of a white solid, mp 82−84 °C. ^{1}H NMR ($CDCl_3$): δ 0.87 (t, J = 7 Hz, 6H, $OCH_2CH_2(CH_2)_5CH_3$), 1.22−1.45 (bm, 20H, $OCH_2CH_2(CH_2)_5CH_3$), 1.75−1.86 (m, 4H, $OCH_2CH_2(CH_2)_5CH_3$), 3.84 (s, 6H, CO_2CH_3), 3.96 (s, 2H, $ArCH_2Ar$), 3.99 (t, J = 6.6 Hz, 4H, $OCH_2CH_2(CH_2)_5CH_3$), 6.81 (d, J = 8.4 Hz, 2H, Ar*H*), 7.82 (s, 2H,), 7.84 (d, J = 8.4 Hz, 2H, Ar*H*).

*4,4′-Dioctyloxy-3,3′-methanediyldibenzoic Acid, **6***. A solution of **5** (2.40 g, 4.44 mmol) in 200 mL of acetone was added to 150 mL of a 3% (w/w) solution of NaOH. The mixture was heated and allowed to stir at reflux for 4 h. After cooling, the solution was acidified to pH 5 with dilute HCl. The white solid which precipitated was collected and washed with water. Recrystallization from ethanol/ethyl acetate (10/1) resulted in 2.05 g (91%) of the desired diacid; mp 211−213 °C. ^{1}H NMR (DMSO-d_6): δ 0.78 (t, J = 6.6 Hz, 6H, $OCH_2CH_2(CH_2)_5CH_3$), 1.21−1.38 (bm, 20H, $OCH_2CH_2(CH_2)_5CH_3$), 1.69−1.78 (m, 4H, $OCH_2CH_2(CH_2)_5CH_3$), 3.87 (s, 2H, $ArCH_2Ar$), 3.96 (t, J = 6 Hz, 4H, $OCH_2CH_2(CH_2)_5CH_3$), 7.00 (d, J = 7.2 Hz, 2H, Ar*H*), 7.66 (s, 2H, Ar*H*), 7.71 (d, J = 7.2 Hz, 2H, Ar*H*).

*4′-((Methoxycarbonyl)oxy)-4-biphenylcarboxylic Acid, **7***. A solution of NaOH (0.80 g, 20.0 mmol) in 20 mL of H_2O was chilled to −5 °C in a three-necked round-bottom flask. 4′-Hydroxy-4-biphenylcarboxylic acid (1.35 g, 6.3 mmol) was dissolved in the solution. Methyl chloroformate (1.0 g, 10.5 mmol) was added dropwise. The resulting solution was stirred at −5 °C for 4 h. The ice bath was removed, and the solution was allowed to warm to room temperature. Concentrated HCl was added until pH 5. A white precipitate formed and was collected on a Büchner funnel. The precipitate was thoroughly washed with water and dried under vacuum at 50 °C. Yield 1.73 g (97%); mp 273−274 °C. ^{1}H NMR (DMSO-d_6): δ 3.86 (s, 3H, OCO_2CH_3), 7.36 (d, J = 8.4 Hz, 2H, Ar*H*), 7.78 (d, J = 8.4 Hz, 2H, Ar*H*), 7.81 (d, J = 8.4 Hz, 2H, Ar*H*), 8.04 (d, J = 8.4 Hz, 2H, Ar*H*). MS (CI+) m/z: 273 (M + 1).

*(S)-1-Methylheptyl 4′-((Methoxycarbonyl)oxy)-4-biphenylcarboxylate, (S)-**8***. 4′-((Methoxycarbonyl)oxy)-4′-biphenylcarboxylic acid, **7** (1.57 g, 5.8 mmol), and triphenylphosphine (2.28 g, 8.7 mmol) were charged to a dried 50 mL round-bottom flask and dried in a vacuum oven at 50 °C for 1 h. The flask was capped with a septum and purged with N_2, and 25 mL of sodium distilled THF was added. The mixture was allowed to stir for 30 min, after which 0.94 g (7.2 mmol) of (*R*)-2-octanol was added. A 50% solution of diethylazodicarboxylate (1.52 g, 8.7 mmol) in THF was added dropwise over a 15-min period. The solution became homogeneous and was allowed to stir at room temperature under a N_2 blanket. After 18 h, the solvent was removed under reduced pressure. The crude oil which resulted was separated by column chromatography using toluene as the eluent. R_f = 0.42. Solvent was removed to yield 1.76 g (80%) of a clear oil. ^{1}H NMR ($CDCl_3$): δ 0.86 (t, J = 6.0 Hz, 3H, $CO_2CH(CH_3)CH_2(CH_2)_4CH_3$), 1.18−1.44 (bm, 11H,

(19) Creed, D.; Gross, J. R. D.; Sullivan, S. L.; Griffin, A. C.; Hoyle, C. E. *Mol. Cryst. Liq. Cryst.* **1987**, *149*, 185.
(20) Griffin, A. C.; Buckley, N. W.; Hughes, W. E.; Wertz, D. L. *Mol. Cryst. Liq. Cryst.* **1980**, *64*, 139.
(21) Hari, U. Novel Dimeric and Siamese Twin Mesogens. Ph.D. Dissertation, University of Southern Mississippi, Hattiesburg, MS, 1991.

$CO_2CH(CH_3)CH_2(CH_2)_4CH_3$), 1.61−1.74 (m, 2H, $CO_2CH(CH_3)CH_2(CH_2)_4CH_3$), 3.91 (s, 3H, OCO_2CH_3), 5.15 (m, 1H, $CO_2CH(CH_3)CH_2(CH_2)_4CH_3$), 7.25 (d, J = 8.6 Hz, 2H, Ar*H*), 7.59 (d, J = 8.6 Hz, 2H, Ar*H*), 7.64 (d, J = 8.6 Hz, 2H, Ar), 8.08 (d, J = 8.6 Hz, 2H, Ar*H*).

*(S)-1-Methylheptyl 4′-Hydroxy-4-biphenylcarboxylate, (S)-**9***. (*S*)-1-Methylheptyl 4′-((methoxycarbonyl)oxy)-4-biphenylcarboxylate, (*S*)-**8** (1.30 g, 3.38 mmol), was dissolved in 20 mL of reagent grade ethanol. Concentrated ammonium hydroxide (10 mL) was added, and the solution was allowed to stir at room temperature for 4 h. The solvent was removed by rotary evaporation under reduced pressure. The crude material was dissolved in CH_2Cl_2 and washed repeatedly with small portions of water until neutral. The organic phase was dried with $MgSO_4$, and the solvent was removed to afford 0.95 g (86%) of a white powder; mp 88−89 °C. ^{1}H NMR ($CDCl_3$): δ 0.87 (t, J = 6.3 Hz, 3H, $CO_2CH(CH_3)CH_2(CH_2)_4CH_3$), 1.28−1.43 (m, 11H, $CO_2CH(CH_3)CH_2(CH_2)_4CH_3$), 1.61−1.78 (m, 2H, $CO_2CH(CH_3)CH_2(CH_2)_4CH_3$), 5.18 (m, 1H, $CO_2CH(CH_3)CH_2(CH_2)_4CH_3$), 6.96 (d, J = 8.4 Hz, 2H, Ar*H*), 7.51 (d, J = 8.4 Hz, 2H, Ar*H*), 7.56 (d, J = 8.4 Hz, 2H, Ar*H*), 8.08 (d, J = 8.4 Hz, 2H, Ar*H*).

*4,4′-Di(octyloxy)-3,3′-methanediyldibenzoic Acid, Bis[(S)-1-methylheptyl 4-biphenylcarboxylate-4′-yl ester], (S,S)-**1***. 4,4′-Di(octyloxy)-3,3′-methanediyldibenzoic acid, **6** (0.75 g, 1.47 mmol), was dissolved in 10 mL of freshly distilled thionyl chloride. The solution was refluxed for 4 h under N_2. Excess thionyl chloride was distilled by normal distillation. FT-IR (KBr) indicated total conversion to the diacyl chloride that was used without further isolation. This compound was dissolved in 5 mL of freshly distilled pyridine and added to a solution of (*S*)-2-methylheptyl 4′-hydroxy-4-biphenylcarboxylate, (*S*)-**9** (1.05 g, 3.23 mmol), in 5 mL of pyridine. The mixture was allowed to stir at room temperature overnight. The solution was poured into 25 mL of 1% (v/v) aqueous HCl. The white precipitate that formed was collected and washed with several small portions of water. The crude material was dried and isolated by column chromatography, first using an eluent of cyclohexane/ethyl acetate (3/1, R_f = 0.85), followed by a second column using toluene (R_f = 0.12). Two recrystallizations from acetone gave the desired product. Yield 1.11 g (67%). ^{1}H NMR (ppm, $CDCl_3$): δ 0.85 (t, J = 6.9 Hz, 6H, $ArOCH_2(CH_2)_6CH_3$), 0.89 (t, J = 6.75 Hz, 6H, $ArCO_2CH(CH_3)(CH_2)_5CH_3$), 1.23−1.92 (bm, 50H, $ArOCH_2(CH_2)_6CH_3$ and $CO_2CH(CH_3)(CH_2)_5CH_3$), 4.04 (t, J = 6.6 Hz, 4H, $ArOCH_2(CH_2)_6CH_3$), 4.06 (s, 2H, $ArCH_2Ar$), 5.18 (m, 2H, $ArCO_2CH(CH_3)(CH_2)_5CH_3$), 6.92 (d, J = 8.4 Hz, 2H, Ar*H*), 7.29 (d, J = 8.7 Hz, 6H, Ar*H*), 7.64−7.67 (m, 8H, Ar*H*), 8.05−8.13 (m, 8H, Ar*H*). $[\alpha]^D_{21}$ = +26°. Anal. Calcd for $C_{73}H_{92}O_{10}$: C, 77.63; H, 8.21. Found: C, 77.61; H, 8.23. MS (CI+) *m*/*z*: 1129 (M + 1). HRMS (CI+) calcd for $C_{73}H_{93}O_{10}$: 1129.67. Found: 1129.68. An analogous sequence of procedures was used to prepare the enantiomer (*R*,*R*)-**1**. $[\alpha]^D_{21}$ = −27°.

*(R)-1-Methylheptyl 4″-((4′-(Octyloxy)benzoyl)oxy)biphenyl-4-carboxylate, (R)-**2***. 4-(Octyloxy)benzoic acid (TCI Chemicals) (0.307 g, 1.23 mmol) and (*R*)-2-methylheptyl 4′-hydroxy-4-biphenylcarboxylate (0.400 g, 1.23 mmol) were dissolved in 25 mL of CH_2Cl_2. EDC-MeI (0.546 g, 1.84 mmol) and DMAP were added dropwise as a solution in 10 mL of CH_2Cl_2. The solution was allowed to stir under N_2 for 18 h. The solution was washed sequentially with water, saturated $NaHCO_3$, and saturated NaCl. The organic phase was dried over $MgSO_4$, and the solvent was removed. The crude material was column chromatographed over silica gel with hexanes/ethyl acetate (9/1, R_f = 0.66) to yield 0.485 g (71%); mp 90−91 °C. ^{1}H NMR ($CDCl_3$): δ 0.82−0.94 (m, 6H, $ArOCH_2(CH_2)_6CH_3$ and $ArCO_2CH(CH_3)(CH_2)_5CH_3$), 1.30−1.85 (m, 25H, $ArOCH_2(CH_2)_6CH_3$ and $CO_2CH(CH_3)(CH_2)_5CH_3$), 4.05 (t, J = 6.3 Hz, 2H, $ArOCH_2(CH_2)_6CH_3$), 5.15−5.21 (m, 1H, $ArCO_2CH(CH_3)(CH_2)_5CH_3$), 6.99 (d, J = 8.7 Hz, 2H, Ar*H*), 7.31 (d, J = 8.4 Hz, 2H, Ar*H*), 7.65 (d, J = 8.4 Hz, 2H, Ar*H*), 7.68 (d, J = 8.7 Hz, 2H, Ar*H*), 8.12 (d, J = 8.4 Hz, 2H, Ar*H*), 8.16 (d, J = 8.4 Hz, 2H, Ar*H*). $[\alpha]^D_{21}$ = −19 °. Anal. Calcd for $C_{36}H_{44}O_5$: C, 77.39; H, 8.30. Found: C, 77.33; H, 8.33. MS (CI+) *m*/*z*: 557 (M + 1).

Characterization Techniques. ^{1}H NMR (300 MHz) spectra were collected on a General Electric QE−300 spectrometer. FT-IR spectra were measured from KBr pellets with a Nicloet Magna-IR spectrometer. Specific rotations were calculated from observed rotations measured in methylene chloride on a Perkin-Elmer 241-MC polarimeter. Mass spectra were measured using a Finnigan MAT TSQ-70 spectrometer. Elemental analyses were performed by Atlantic Microlabs of Norcross, GA.

A Perkin-Elmer Series-7 thermal analysis system was used for differential scanning calorimetry (DSC) measurements. A scan rate of 2 °C/min was used for all DSC analyses. Transition temperatures reported are the peak values, taken on the first cooling cycle. An Olympus BX60 microscope in conjunction with a Mettler FP82HT hot stage and FP90 central processor was used for temperature-controlled polarized optical microscopy. Samples for POM were prepared by heating the materials above their clearing temperatures on untreated glass slides and allowing capillary action to fill the space between the slides and untreated glass cover slips.

Polarization measurements were performed on a custom-made analysis system. The samples were introduced into either 4-μm-spaced Displaytech parallel-rubbed ITO (indium tin oxide) coated glass cells or custom-made cells of various thickness, by capillary action, as above. Waveforms were generated using a custom-written LabView (National Instruments) operating program. The signal was amplified by a Kepco BOP 500M bipolar operational amplifier. The cell response current was converted to a voltage and amplified by a Keithley 427 transimpedance amplifier. The resulting signal was fed back to the PC and read by a LabView data acquisition program. Integration of the current response provides the polarization. A modification to this system allowed for response time measurements. The sample cell, in the hot stage, was positioned in the focused, plane-polarized beam of a Uniphase 1507-0 HeNe Laser. The transmitted intensity of the beam was measured by a UDT Sensors UV100 photodiode array after passing through a crossed polarizer. The current signal from the photodiode was then converted to a voltage and amplified, as above, and read into the PC with LabView.

Results and Discussion

Synthesis. The fundamental structural characteristics necessary for compounds to exhibit ferroelectric and antiferroelectric behavior have been widely investigated.[4,8,9] We have developed dimeric analogues of these compounds which are laterally linked through methylene spacers. The mesogenic structure is based on the fundamental components common to previously reported antiferroelectric liquid crystals (AFLCs): two rigid central cores linked through a spacer moiety, with two terminal, flexible alkyl chains, one of which possesses an asymmetric carbon.[8]

The convergent synthetic pathway used to prepare dimer **1** is outlined in Scheme 1 and is analogous to those outlined by J. W. Goodby and co-workers.[8,9] The dimerization of methyl 4-hydroxybenzoate was achieved by condensation of an excess of this reagent with formaldehyde under acidic aqueous conditions.[22] The bisphenol, **4**, was etherified with 1-iodooctane in the presence of K_2CO_3. Saponification of the methyl esters of **5** followed by acidification provided the dietherified dicarboxylic acid, **6**. The chiral rigid core of the molecule, **9**, was synthesized by first protecting 4′-hydroxy-4-biphenylcarboxylic acid as the methyl carbonate, **7**. Anhydride formation was prevented by using a decreased reaction temperature. The carboxylic acid

(22) Hirao, I.; Tokunaga, S.; Hironaga, M. *Nippon Kagaku Kaishi* **1978**, *12*, 1723.

Scheme 1

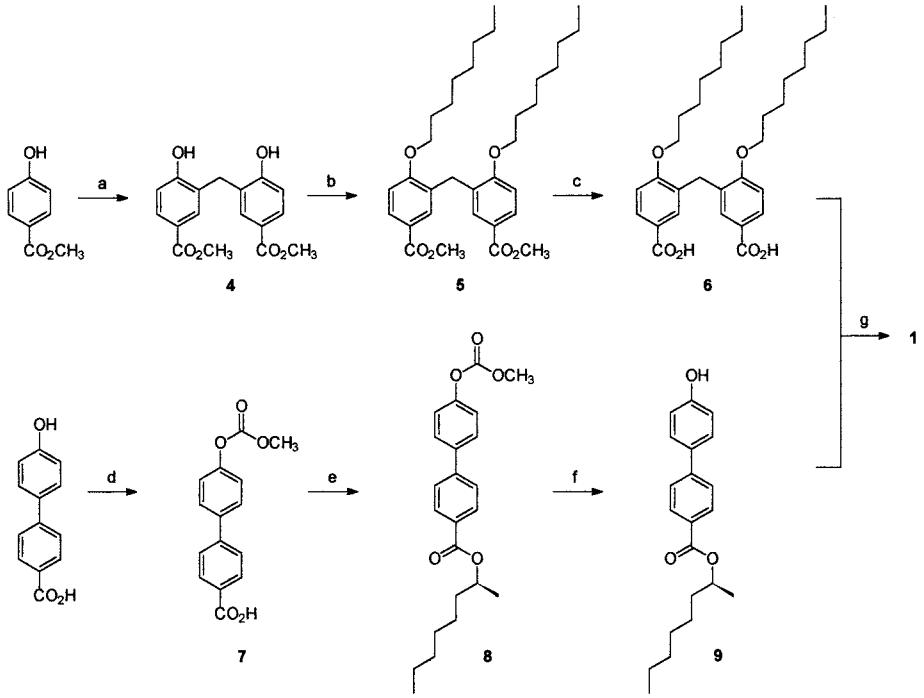

[a] CH_2O, H_2SO_4, H_2O. b: $CH_3(CH_2)_7I$, K_2CO_3. c: NaOH, H_2O, HCl. d: CH_3OCOCl, NaOH, H_2O, HCl. e: (*R*)-2-octanol, DEAD, Ph_3P; NH_4Oh, CH_3CH_2OH. f: $SOCl_2$, Pyr.

functionality was esterified using enantiomerically pure secondary alcohols under Mitsunobu[23] conditions. This transformation led to complete inversion of stereochemistry in the ester, **8**. The carbonate was cleaved under mild basic conditions to give the free phenol. Final esterification between the optically active hydroxy−biphenyl derivative, **9**, and the dicarboxylic core, **6**, was accomplished via the diacyl chloride which was prepared by reaction with thionyl chloride. The monomeric counterpart, **2**, was prepared from the chiral biphenyl compound, **9**, and commercially available 4-(octyloxy)-benzoic acid, using 1-(3-dimethylaminopropyl)-3-ethylcarbodiimide methiodide, EDC-MeI, as a coupling agent. It should be noted that the milder carbodiimide coupling procedure used for the final esterification of the monomeric compound **2** was not a successful method for preparing the dimer **1**. The mono-*N*-acyl derivatives of compound **6** and the carbodiimides tested (DCC, DIC, EDC-MeI) were found to be the major products of the reactions.

Thermal Microscopy and Calorimetry. Differential scanning calorimetry (DSC) and polarized optical microscopy (POM) were employed to determine transition temperatures and to estimate phase assignments.[24] Electrooptic response provided further insight into the nature of the observed phases and is the topic of the subsequent section.

A DSC thermogram of compound **1** is shown in Figure 2a. A monotropic K to K transition and a crystal to LC transition are observed upon first heating, in addition to a well-defined clearing point of 158 °C. The cooling trace reveals a supercooled region persistent to the crystallization at 91 °C. As can be seen in the expanded thermogram in Figure 2b, several small transitions are observable upon cooling between the clearing and crystallization temperatures. Both fan focal conic and homeotropic textures are observed within the various mesophases, as shown in the polarized optical micrographs of Figure 3. The first mesophase below the isotropic state was assigned chiral smectic A (S_A*), on the basis of the smoothness of the focal conic region observed by POM using transmitted light, as in Figure 3a, taken at 135 °C. When observed with reflected polarized light, no iridescence is seen in the homeotropically aligned areas, consistent with a nonhelical structure expected for S_A*.

Subsequent cooling below 131 °C leads to the appearance of a grooved-like texture on the focal conic surface, consistent with the onset of a tilted smectic C phase, S_C*. As the temperature is decreased, a moving planar texture, commonly identified with ferrielectric S_C* phases,[12,14] is exhibited in the homeotropic regimes. The phenomenon is clearly observed by POM but does not reproduce well in photomicrographs. The planar texture, along with an increase in the graininess of the focal conic, is evident over an approximately 8° temperature range that corresponds to the region of the low-enthalpy transitions observed by DSC, 124−116 °C. On the basis of these data, the two mesophases within this temperature range have been tentatively assigned as ferrielectric phases, although no discernible, abrupt transitions between these phases is observed by POM.

The disappearance of the planar texture is noted at approximately 116 °C, accompanied by an increase of bandedness in the focal conic areas, as shown in Figure 3b, taken at 100 °C. These bands are evidence of a helical arrangement; however, no iridescence is observable with reflected polarized light in the homeotropic

(23) (a) Mitsunobu, O. *Synthesis* **1981**, 1. (b) Mitsunobu, O.; Eguchi, M. *Bull. Chem. Soc. Jpn.* **1971**, *44*, 3427.

(24) Gray, G. W.; Goodby, J. W. *Smectic Liquid Crystals, Textures and Structures*; Hill: London, 1984.

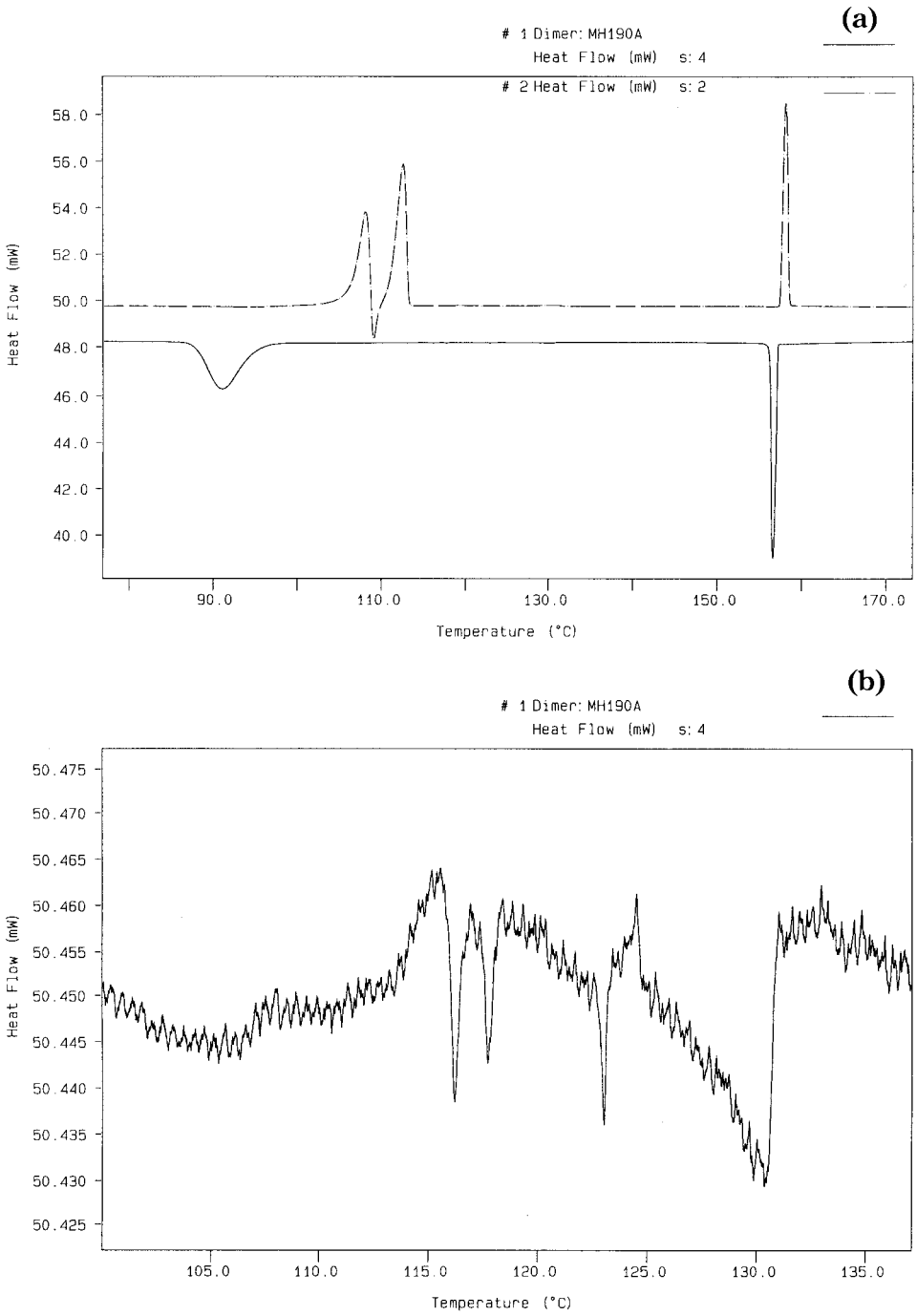

Figure 2. DSC thermograms. (a) Dimer **1**, 2 °C/min. (b) Expanded region showing multiple transitions.

regions. This may result from a helical pitch length beyond visible wavelengths.

The transition temperatures of the monomer, **2**, and MHPOBC, **3**, have been previously reported in the literature.[8,10] Our thermal and optical analyses of these compounds correspond well with the established values. Additionally, DSC of compound **2** shows a previously unreported recrystallization from supercooled S_C* at 63 °C. Due to the kinetic nature of this phenomenon, the temperature of recrystallization is largely dependent on both scan rate and the nature of sample. Therefore, variation in its value is not unexpected. Scheme 2 summarizes the preliminary phase transitions for the three compounds based on DSC, POM, and electrooptic analyses (vide infra).

Electric Field Studies. The triangular wave method described by Takezoe, Fukuda, and co-workers[25] was used to investigate the polarization response of these materials. The initial studies were performed using the commercially available 4-μm-spaced, unidirectionally rubbed glass cells with ITO electrodes. Upon cooling from isotropic, no observable spontaneous polarization is detected in the S_A* phase. However, the electroclinic effect is evident, which further supports the assignment of this mesophase.

Figure 4 shows the polarization current response of dimer **1** to an applied voltage of 45 V/μm at 1 Hz as a

(25) Miyasato, K.; Abe, S.; Takezoe, H.; Fukuda, A.; Kuze, E. *Jpn. J. Appl. Phys.* **1983**, *22*, L661.

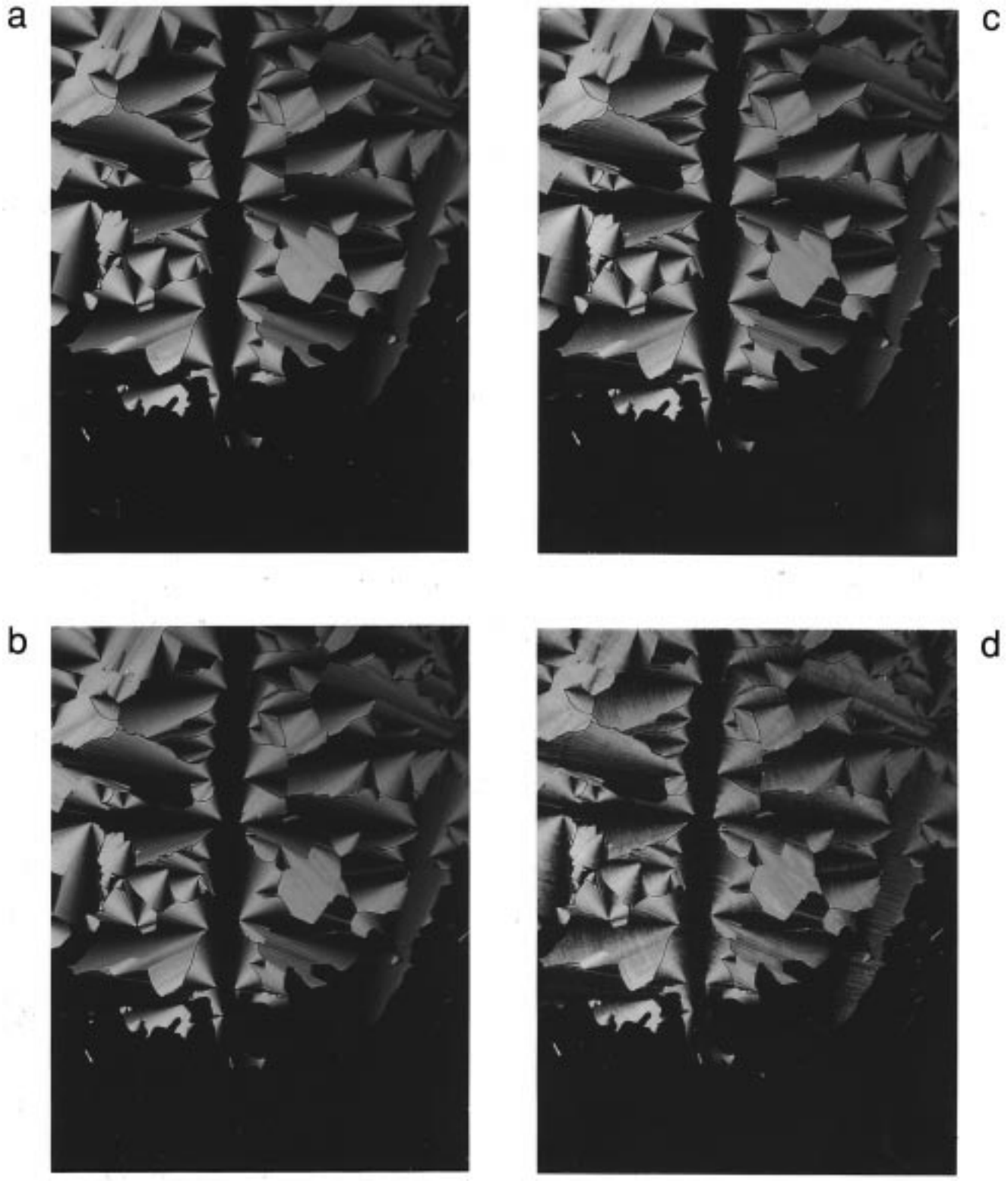

Figure 3. Polarized optical micrographs of **1** in focal conic and homeotropic alignments. (a) S_A*, 135 °C. (b) S_{C3}*, 100 °C. Magnification = 75X.

function of temperature within the remaining smectic mesophases. Upon cooling from the S_A* phase (129 °C), a polarization current consisting of two peaks per half-cycle is observed. This is indicative of tristable switching, and integration of this signal results in a double hysteresis, characteristic of an antiferroelectric phase, AF. Unlike MHPOBC, **3**, that shows definitive field response behavior within each of its many mesophases,[10,11] dimer **1** shows no clear response changes which correlate directly with observed transitions in either DSC or POM. Instead, there is a gradual transition from a doubly to a singly peaked current response. This is clearly demonstrated in Figure 4 where, as the temperature decreases, the size of the second peak diminishes as the first one increases. There is a temperature range from 124 to 116 °C which

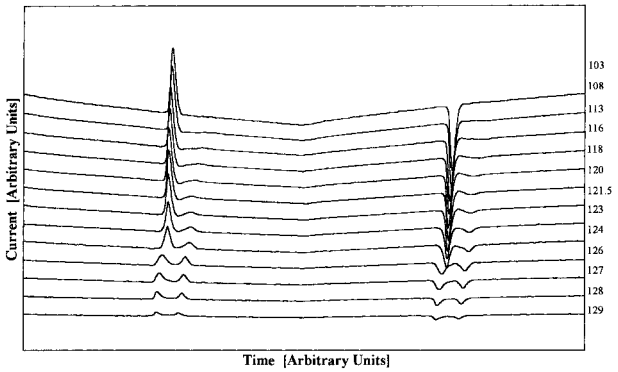

Figure 4. Polarization current response of **1** to an applied field of 45 V/μm as a function of temperature (°C on left *y*-axis). Measurements were made at 1 Hz.

Scheme 2. Polymorphism As Determined By DSC and POM

1: I $\xrightarrow{157}$ S_A* $\xrightarrow{131}$ AF $\xrightarrow{124}$ S_C*$_1$ $\xrightarrow{118}$ S_C*$_2$ $\xrightarrow{116}$ S_C*$_3$ $\xrightarrow{91}$ K

2: I $\xrightarrow{129}$ S_A* $\xrightarrow{82}$ S_C* $\xrightarrow{63}$ K

3: I $\xrightarrow{148}$ S_A* $\xrightarrow{122}$ S_C*$_\alpha$ $\xrightarrow{120.9}$ S_C* $\xrightarrow{119.2}$ S_C*$_\gamma$ $\xrightarrow{118.4}$ S_C*$_A$ $\xrightarrow{84}$ K

encompasses two mesophases where nonsymmetric switching is observed. This may be attributed to ferrielectric-type arrangements with intermediate degrees of polarization cancellation between layers. At the lower temperatures, only a single peak is observed per half-cycle, consistent with a single hysteresis and a ferroelectric phase, S_C*.

This gradient of polarization responses from two to one peak has been demonstrated before in a compound of the homologous series of monomer **2**.[8] However, the sequence of apparent antiferro- to ferri- to ferroelectric behavior with decreasing temperature is not commonly observed. In fact, the opposite trend is regarded to be the universal phase order for tilted smectic materials which exhibit all three phases, including MHPOBC, **3**.[7,12,26] A subtle transition from antiferroelectric switching to ferroelectric switching upon cooling has been observed in S_C*$_\alpha$ phases,[7] and may be the cause of the unusual behavior.

Further investigation of these materials by POM at temperatures where a single polarization peak is observed demonstrates more anomalous behavior. For example, at 115 °C, POM under an applied field shows the presence of three switching states as shown in Figure 5. Close inspection of individual domains within the polydomainal focal conic texture shows these three states. The areas of the material which appear dark under a positive applied field appear bright under a corresponding negative field, whereas in the absence of a field, a clear distinction is observed. This is not consistent with the single-hysteretic behavior generally ascribed to a ferroelectric S_C* phase.

A possible explanation for this unusual behavior could be attributed to the field-induced unwinding of a helical smectic structure. The application of a field can unwind the thermodynamically favored helix, resulting in a bookshelf geometry.[6] The direction of the polarization is dictated by the sign of the applied field, and thus, two energetically degenerate states can be induced. To probe this possibility, we mechanically unwound the helix and observed the field-induced effect by POM. Although a monodomain bookshelf geometry could not be attained within the commercial cells, we were able to unwind the helical structure by a combination of surface treatment and shearing of custom-made cells[27]

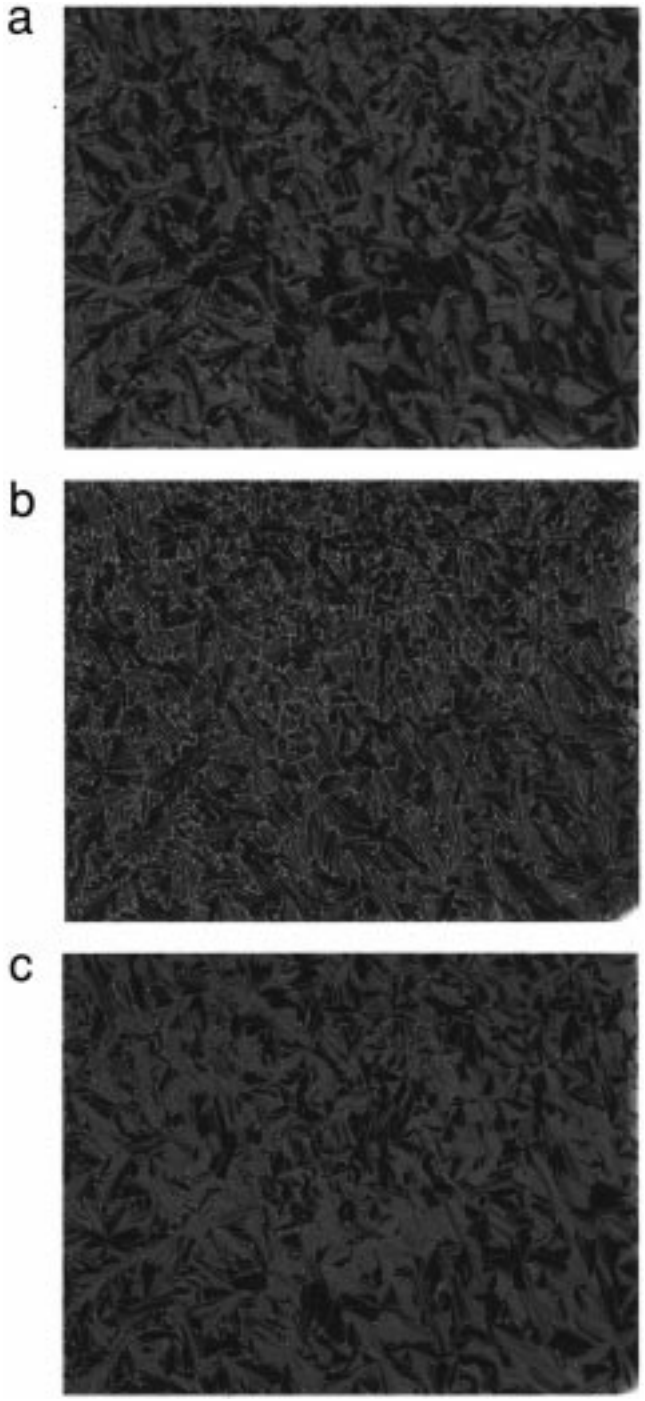

Figure 5. Polarized optical micrographs showing switching of **1** in focal conic arrangement upon application of field. (a) +27.5 V/μm; (b) 0 V/μm; (c) −27.5 V/μm. Magnification = 60X.

(26) Takanishi, Y.; Hiraoka, K.; Agrawal, V. K.; Takezoe, H.; Fukuda, A.; Matsushita, M. *Jpn. J. Appl. Phys.* **1991**, *30*, 2023.

(27) Rieker, T. P. The Layer and Director Structures of Ferroelectric Liquid Crystal Cells. Ph.D. Dissertation, University of Colorado, Boulder, CO, 1988.

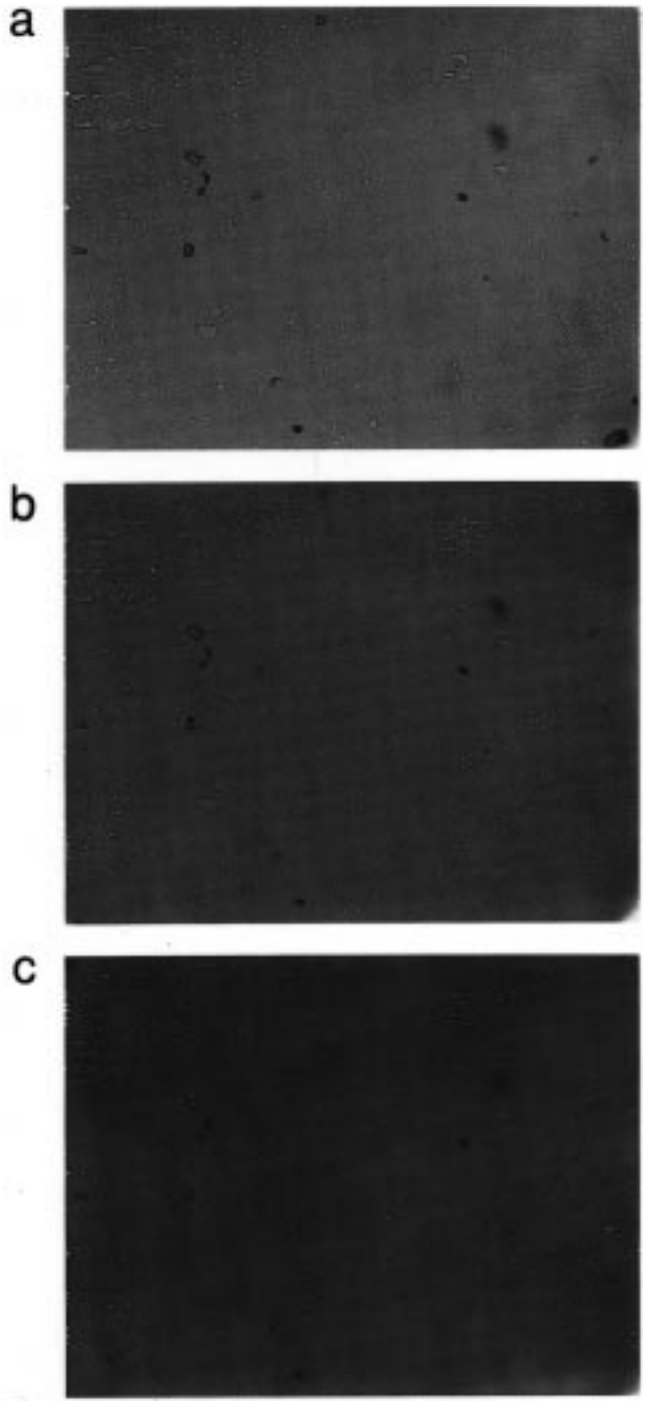

Figure 6. Polarized optical micrographs showing switching of **1** in an unwound, bookshelf monodomain upon application of field. (a) +12.5 V/μm; (b) 0 V/μm; (c) −12.5 V/μm. Magnification = 60X.

under an applied field at a temperature just below the clearing point. As shown in Figure 6, tristable switching is again apparent. Therefore, we conclude that helix unwinding is not responsible for the three optical states observed in this phase that exhibits only a single polarization peak. X-ray diffraction studies are intended to assist in deciphering the mechanism by which this peculiar switching occurs.

Direct comparison of the temperature dependence of the polarization responses of dimer, **1**, and monomer, **2**, as shown in Figure 7, indicates that both molecules follow a typical increase in polarization magnitude as

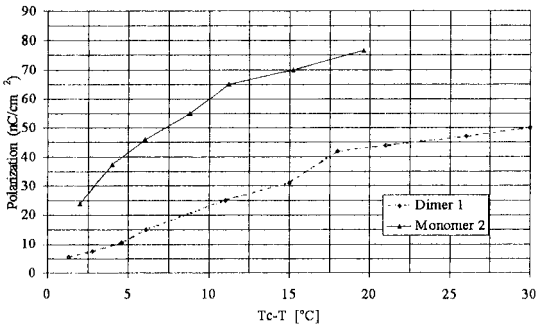

Figure 7. Polarization as a function of reduced temperature for **1** and **2** in aligned samples. Measurements made on samples in the focal conic alignment showed nearly identical values.

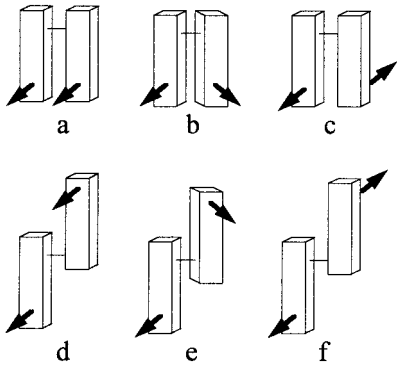

Figure 8. Possible molecular conformations of dimer **1** in parallel (a−c) and antiparallel (d−f) arrangements. Arrows represent direction of orthogonal dipole moment.

the temperature decreases from the Curie point, T_C. This is generally ascribed to an increase in tilt angle and a corresponding increase in asymmetry. As symmetry is broken, free rotation of individual mesogens is diminished, favoring dipole alignment. There is also a concurrent increase in the viscosity of the material. The higher polarization values found for the monomer **2** were unexpected. Our initial prediction was that the dimer would have higher polarizations due to the incorporation of a covalent linkage which would mandate alignment of dipoles of the two halves of the compound. The higher viscosity expected for **1** would also lend to higher polarization values.

Since the effective dipole moment per mesogenic unit is essentially equal between compounds **1** and **2**, some mode of dipole cancellation must be involved in the packing arrangement of the dimer which does not exist for the monomer. A variety of different models can be proposed which may explain the observed behavior. These are shown schematically in Figure 8. A parallel conformation of dimer halves may lead to completely aligned dipoles (Figure 8a), dipoles which are skewed, (Figure 8b), or dipoles which cancel (Figure 8c). An antiparallel arrangement, can be envisioned to result in analogous states (Figure 8d−f). Clearly, these models are oversimplified. However, the intent is to indicate the multitude of molecular dipole arrangements which can arise in different conformations of dimers having this type of architecture. If one then considers the lamellar structure of the smectogens, even more possibilities arise, including bilayers and interdigitation. Other research groups have proposed similar confor-

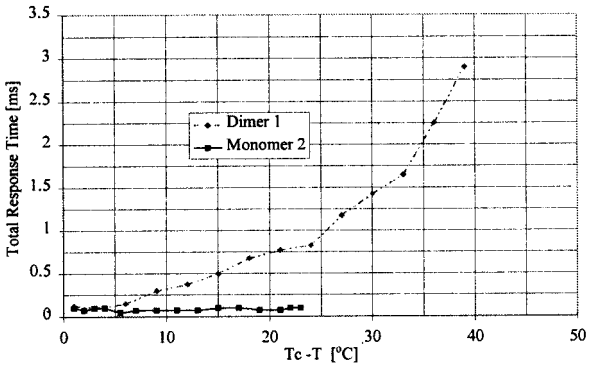

Figure 9. Total response time as a function of reduced temperature for **1** and **2** in aligned samples. As with the polarization measurements, no noticeable difference was detected between monodomain samples and those in focal conic alignment.

mational possibilities in laterally linked dimers.[18−21,28] In addition, others, investigating head-to-tail electrooptic dimers,[18,29−31] have suggested comparable models. Again, our intention is to use X-ray diffraction studies as a means of determining molecular conformations by examining layer spacing.

The response time as a function of reduced temperature for compounds **1** and **2** is shown in Figure 9. This reported total response time was determined as the sum of the lag time and the actual switch time.[32] The slower response time of the dimer **1** is consistent with the previously mentioned higher viscosity expected for this material compared to **2**. Unlike the monomer **2** whose response time shows little dependence on temperature, the rate of switching of dimer **1** is highly temperature dependent.

Conclusion

Laterally linked dimeric liquid crystals that exhibit tilted smectic phases have been designed and synthesized. The polymorphism and electrooptic properties of the dimer vary dramatically with the corresponding monomer. The dimers exhibit bistable and tristable switching within these tilted smectic phases. The absolute identification of the individual mesophases has proven difficult, as switching characteristics vary from those of previously reported ferroelectric and antiferroelectric materials. Most notable of these differences is the observation of optical tristability within two different temperature regimes: one, at higher temperatures, where the material exhibits a double-hysteretic response to an applied electric field, and the other that shows a single hysteresis and exists at lower temperatures. The mechanism by which this switching behavior occurs is unclear but is the subject of current studies. The variety of proposed parallel, antiparallel, and interdigitated alignment states, and the field-induced reorientation between these states, offer a multitude of possibilities to describe this unusual behavior. X-ray diffraction studies at variable temperature and applied field strength should help to elucidate these phenomena.

These materials also may be useful in providing insight toward the mechanism by which antiferroelectricity arises in liquid crystal media, by providing a system where so-called "dipole moment pairs"[7,18] are covalently linked within the same molecule. Toward this end, we are preparing the diastereomeric meso analogue of **1**, as well as other related compounds, to investigate the effect that stereochemistry has on the electrooptic behavior of laterally ligated twin liquid crystals.

Acknowledgment. We wish to thank Dr. Robert Twieg, Dr. Do Yoon, and Dr. U. Paul Schröder of the IBM Almaden Research Center and Dr. David Walba and Dr. Renfan Shao of the University of Colorado at Boulder for their insightful discussions and assistance in these studies. D.R.M. is grateful to the Eastman Kodak Company for providing him with an Eastman Kodak Fellowship.

CM970764M

(28) Andersch, J.; Tschierske, C.; Diele, S.; Lose, D. *J. Mater. Chem.* **1996**, *6*, 1297.
(29) Shilov, S. V.; Skupin, H.; Kremer, F.; Wittig, T.; Zentel, R. *Macromol. Symp.* **1997**, *119*, 261.
(30) (a) Suzuki, Y.; Isozaki, T.; Kusumoto, T.; Hiyama, T. *Chem. Lett.* **1995**, 719. (b) Suzuki, Y.; Isozaki, T.; Hashimoto, S.; Kusumoto, T.; Hiyama, T.; Takanishi, Y.; Takazoe, H.; Fukuda, A. *J. Mater. Chem.* **1996**, *6*, 753.
(31) Robinson, W. K.; Kloess, P. S.; Carboni, C.; Coles, H. J. *Liq. Cryst.* **1997**, *23*, 309.
(32) Twieg, R. J.; Betterton, K.; Nguyen, H. T.; Tang, W.; Hinsberg, W. *Ferroelectrics* **1989**, *91*, 243.